Laser interference structuring of *a*-Ge films on GaAs

P. V. Santos[a)]
Paul-Drude-Institut, Hausvogteiplatz 5-7, 10117 Berlin, Germany

A. R. Zanatta
Instituto de Física de São Carlos, USP, São Carlos 13560-250, São Paulo, Brazil

U. Jahn and A. Trampert
Paul-Drude-Institut, Hausvogteiplatz 5-7, 10117 Berlin, Germany

F. Dondeo and I. Chambouleyron
Instituto de Física Gleb Wataghin, UNICAMP, Campinas 13083-970, São Paulo, Brazil

(Received 25 September 2001; accepted for publication 7 December 2001)

We have investigated the laser interference crystallization (LIC) of amorphous germanium films on (100)-oriented GaAs substrates using nanosecond laser pulses. We demonstrate that LIC can produce periodic arrays of epitaxially crystallized Ge lines on GaAs with submicrometer widths. The gratings display a surface undulation with faceted surfaces, which depends on laser fluency. The undulation is attributed to the lateral solidification process induced by the temperature gradients created during the LIC process. © *2002 American Institute of Physics.* [DOI: 10.1063/1.1448674]

I. INTRODUCTION

Pulsed laser crystallization of amorphous films has been extensively used for the fabrication of large area polycrystalline films of electronic quality on low-cost substrates.[1] When used in an interference configuration [laser interference crystallization (LIC^2)], laser crystallization becomes a structuring technique capable of producing microstructures of crystalline materials with submicrometer dimensions. In LIC, two or three coherent and pulsed laser beams are brought to interfere on the surface of an amorphous film. The strong light intensity around the maxima of the interference pattern leads to the selective heating and crystallization of the amorphous material around these regions. LIC allows for the fabrication of periodic structures in a ns time scale without the need for lithography. It has been employed to fabricate arrays of lines or of dots of polycrystalline silicon[2–4] and polycrystalline germanium[5] on glass substrates as well as for the structuring of crystalline GaAs/(Al,Ga)As multilayers.[6] The lateral temperature gradient induced by the selective illumination has also been applied to induce a lateral solidification of amorphous silicon films, which permits the control of grain size and orientation of the crystallized material.[3,4,7,8]

In a previous work,[9] we have demonstrated that amorphous (*a*-) Ge films deposited on crystalline GaAs substrates can be epitaxially crystallized when irradiated by short laser pulses. The Ge/GaAs system is ideal for laser crystallization studies since the two materials are almost perfectly matched with respect to lattice constants and thermal expansion coefficients. In addition, they are thermodynamically immiscible,[10] so that the formation of a $(GaAs)_{1-x}Ge_{2x}$ interface alloy should be inhibited under equilibrium conditions. We found, however, that the fast cooling rates after laser irradiation may lead to the formation of a nonequilibrium $(GaAs)_{1-x}Ge_{2x}$ alloy at the interface between the Ge and the GaAs film.[9]

In this work we investigate the LIC of *a*-Ge films grown on (100)-oriented crystalline GaAs substrates. We demonstrate that submicrometer lines of epitaxial Ge on GaAs can be produced by the LIC technique by using single pulses from a frequency-doubled Nd-YAG laser. The crystallization process was investigated by combining atomic force microscopy (AFM), transmission electron microscopy (TEM), and scanning electron microscopy (SEM). An interesting feature of the LIC Ge lines is that they exhibit a triangular cross section with well-defined faceted surfaces. The surface undulation indicates that a considerable amount of material is transported in the direction parallel to the surface during the laser treatment. The faceted undulation is attributed to the lateral epitaxial solidification process induced by the temperature gradient created by the laser interference pattern. Possible applications of the laser crystallized lines include lateral Ge/GaAs heterojuctions for light detection in the 1.3–1.5 μm wavelength region.

This work is organized as follows. In Sec. II we describe the procedures involved in the preparation and in the characterization of the samples. The experimental results on LIC are presented in Sec. III and discussed in Sec. IV, where a model for the crystallization process is presented.

II. EXPERIMENTAL DETAILS

The samples used in the present studies consist of 100-nm-thick *a*-Ge films deposited on (100)-oriented GaAs by ion-beam-assisted sputtering. The system used for the deposition and the deposition procedure are described in detail in Refs. 9 and 11. The crystallization experiments were performed using single pulses (pulse width of ~7 ns) from a frequency-doubled Nd:YAG laser ($\lambda_L = 532$ nm).[9] The laser beam profile was homogenized using a vacuum spatial filter, leading to a Gaussian-like intensity profile with a diameter

a)Electronic mail: santos@pdi-berlin.de

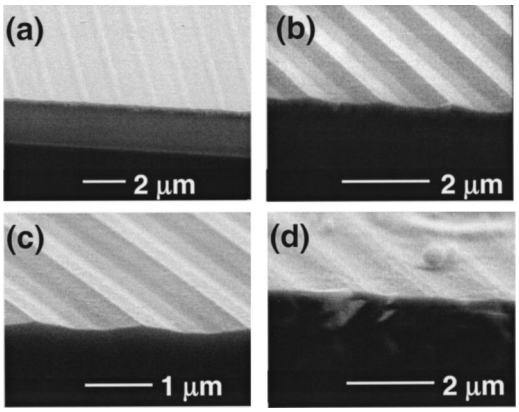

FIG. 1. Scanning electron micrographs of LIC Ge lines on GaAs produced using (a) low, (b) and (c) moderate, and (d) high laser fluencies. The micrographs were recorded at different positions on the spot with a diameter of ~4 mm created on the sample surface by LIC using an average laser fluency of 70 mJ/cm^2.

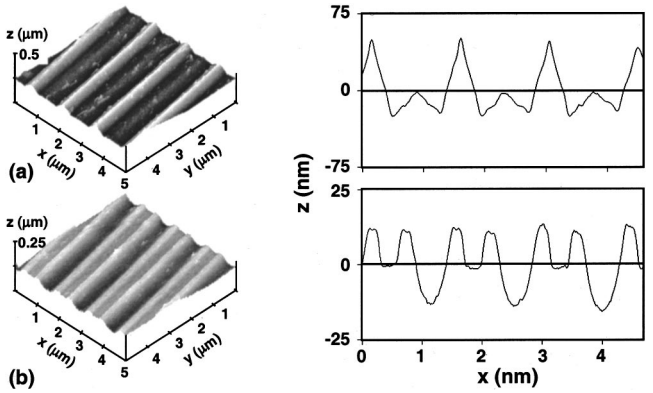

FIG. 2. Atomic force micrographs (left panel) and surface profiles (right panel) of line gratings corresponding to the SEM micrographs in (a) Fig. 1(c) and (b) Fig. 1(d), respectively.

$\phi_0 \sim 4$ mm on the sample surface. The integrated intensity of the laser pulses was adjusted using an attenuator consisting of a half wave plate and a polarizer and measured by deviating a portion of the laser beam to a detector. From the integrated intensity and from the diameter of the laser spot we determined the average fluency E_p over the sample surface. The laser exposures were carried out in air and at room temperature.

The LIC experiments were performed by splitting the spatially filtered laser beam into two beams of equal intensity, which impinged on the sample under an angle of incidence θ.[2] The difference in optical path length of the two beams was kept below the coherence length of the laser of ~1 cm. The grating period d is related to the laser wavelength and to the angle θ by $d=\lambda_L/(2\sin\theta)$.[2] Most of the experiments were performed with $\theta=10°$ so as to yield a lateral period $d=1.5\,\mu$m. The structural properties of the crystallized samples were investigated using SEM, AFM, and cross-sectional TEM.

III. RESULTS

Figure 1 displays SEM micrographs of gratings formed on a-Ge films on GaAs by the LIC process using an integrated laser fluency $E_P=70$ mJ/cm^2. This fluency is sufficiently high to completely melt and crystallize the a-Ge film at the center of the laser spot. The micrographs in Figs. 1(a)–1(d) were recorded at different radial distances from the center of the laser spot, corresponding to regions of progressively larger local laser fluencies. The light interference pattern was oriented close to a ⟨011⟩ surface direction. The micrographs were recorded after cleaving the samples to expose a {011} cleavage plane, in order to allow for the observation of the cross section of the crystallized lines.

For low laser fluencies [Fig. 1(a)], only a small region of the a-Ge around the maxima of the light interference fringes melts and subsequently crystallizes in the form of lines with a round cross section. The width of the crystallized lines increases with laser fluency. Simultaneously, their cross-sections develop a triangular shape due to the formation of faceted surfaces [Figs. 1(b) and 1(c)]. As the fluency is further increased, the cross section changes from triangular to trapezoidal-like [Fig. 1(d)].

Details of the surface morphology of gratings crystallized using moderate [corresponding to Fig. 1(c)] and high laser fluencies [Fig. 1(d)] are illustrated in the AFM micrographs in the left panels of Figs. 2(a) and 2(b), respectively. The corresponding profiles of the surface relief measured along a direction perpendicular to the lines are displayed in right panels. The surface profiles in Fig. 2(a) are almost perfectly triangular. If we neglect the small misalignment of the lines with respect to the ⟨011⟩ direction, the faceted sides of the lines correspond approximately to a $[n11]$ surface with $n=3$. The height of ~70 nm of the triangular lines in Fig. 2(a) is almost as large as the original thickness of the a-Ge film of 100 nm. For higher fluencies, the amplitude of the surface undulation reduces considerably. The cross section of the lines becomes trapezoidal-like. The oblique sides of the trapezoids may also be faceted: those in Fig. 2(b) (right panel) correspond to a faceted surface with n in the range from 3 to 6. In addition, the central region of the lines are depressed with respect to the surroundings.

A cross-sectional SEM micrograph of the LIC gratings produced using a moderate fluency is illustrated in Fig. 3. The fluency in this case was high enough to melt the Ge film over the whole surface area, and also the GaAs substrate, at the positions close to the interference maxima (the melting temperature of GaAs, of 1513 K, is 300 K higher than that of crystalline Ge;[12] the crystallization temperature of a-Ge films depends on the deposition conditions and normally lies between 783 and 863 K).[13,14] The interdiffusion of film and substrate materials leads to the formation of a nonequilibrium $(GaAs)_{1-x}Ge_{2x}$ alloy at the film–substrate interface after solidification.[9] As a result, the interface becomes less well-defined close the positions of the interference maxima (indicated by the arrow d_1). The micrograph was recorded using an in-lens detector in order to enhance the compositional contrast between the Ge overlayer and the substrate. The SEM contrast seems to be associated not only with the normal difference in contrast between Ge and GaAs, but also with modification of the GaAs work function by Ge interdiffusion and doping.[15] The thickness of the surface film in Fig.

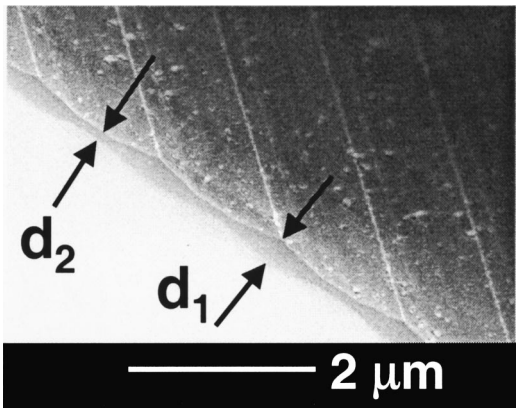

FIG. 3. Cross-sectional SEM micrograph of a grating formed using a moderate laser fluency [corresponding to Fig. 1(b)]. The micrograph was recorded under an observation angle of 30° with respect to the normal to the cleaved edge.

3 becomes modulated with the periodicity of the light interference pattern. The values $d_1 = 224$ nm and $d_2 = 64$ nm for the film thickness at the maxima and minima of the light interference pattern are substantially larger and smaller, respectively, than the original thickness of the a-Ge film of 100 nm. The reduction in film thickness at the interference minima indicates that the crystallization is accompanied by a considerable amount of material transport along the surface.

The microscopic structure of the LIC gratings was further investigated using TEM. Figures 4(a) and 4(b) compare cross-sectional TEM micrographs of gratings produced using low and moderate laser fluencies, respectively. For the TEM analysis, the two gratings were glued to each other using an epoxy (white region). In both figures the Ge film melted completely only around the interference maxima (region I), where it subsequently crystallized as a single crystal epitaxial layer. The width of the epitaxial lines increases with laser fluency. Note that only the grating in Fig. 4(b) displays a faceted surface with triangular morphology, thus indicating that faceting requires a laser fluency higher than that necessary for epitaxial crystallization.

Around the interference minima (region II in Fig. 4), the Ge layer either remains amorphous or crystallizes with a high density of planar defects. Structural details of the transition region between the epitaxial (region I) and the defect-rich Ge areas (region II) are illustrated in Fig. 5. The dark line along the Ge/GaAs interface is attributed to the presence of residual impurities (in the submonolayer range) on the

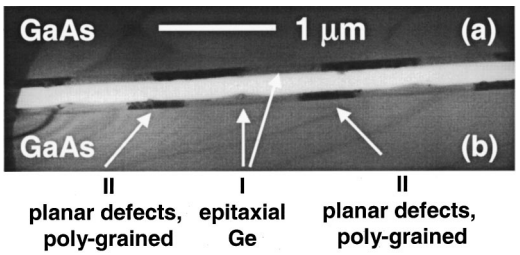

FIG. 4. TEM micrograph of LIC Ge/GaAs gratings produced using (a) low and (b) moderate laser fluencies. For the TEM measurements, the Ge/GaAs structures were glued against each other using an epoxy (white area).

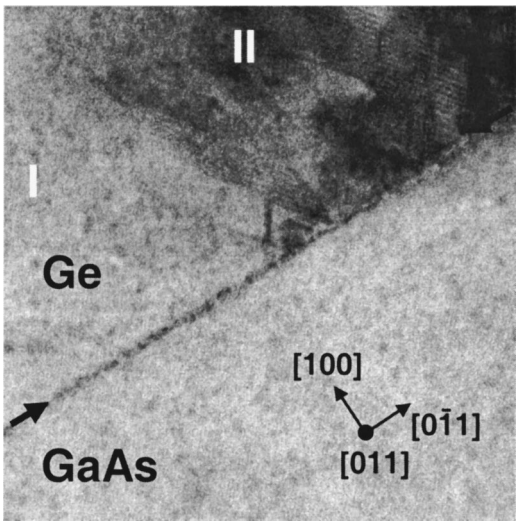

FIG. 5. Details of the lateral interface between the epitaxial (region I) and polycrystalline areas (region II) of LIC Ge/GaAs gratings. The defects in region II consist of twins and stacking faults oriented along {111} planes.

surface of the GaAs wafers prior to the Ge deposition, which remain trapped at the interface after the crystallization process. The low impurity concentration does not disturb the perfect atomic alignment across the interface after laser crystallization.[9,16] In fact, no structural defects like dislocations or stacking faults were detected in region I, as expected for perfect epitaxial growth on a lattice matched substrate. The transition between regions I and II is characterized by extended defects consisting mainly of twins and stacking faults oriented along the $\langle 111 \rangle$ direction. It is interesting to note that the strain contrast associated with these structural defects is confined to region II and does not extend to region I or to the substrate.

Faceted surfaces were not observed on regions of the GaAs substrates not covered by the a-Ge film, when they are irradiated with the same laser interference pattern. This result indicates that faceting requires the presence of the a-Ge film. In order to investigate the influence of the period of the light interference pattern on the morphology of the LIC lines, gratings were also prepared using a smaller period $d = 0.5\,\mu$m. The surface of the short period gratings are only weakly undulated with an undulation amplitude ($\sim$15 nm) much smaller than the thickness of the original a-Ge film. No well-defined faceting was observed in this case.

IV. DISCUSSION AND CONCLUSIONS

The results of the previous section demonstrate that LIC can be applied for the fabrication of submicron lines of Ge on GaAs. The structure and morphology of the LIC lines depend strongly on laser fluency. For low fluencies, only the surface portion of the a-Ge material close to the interference maxima melts. The melt then crystallizes in the polycrystalline phase yielding a convex surface profile [cf. Fig. 1(a)]. Fluencies high enough to melt the Ge film down to the interface with the substrate lead to single crystal lines with planar surfaces. The lines are separated from each other by stripes of amorphous or polycrystalline material, as indicated

in Fig. 4(a). When the fluency is further increased, lines fabricated using an interference period of 1.5 μm develop a triangular cross section with faceted surfaces, as illustrated in Figs. 2(a) and 4(b). Higher fluencies lead to a reduction in amplitude of the surface undulation [cf. Fig. 1(d)]. We note that faceting has not been observed in *a*-Ge films crystallized with a single laser beam,[9] thus indicating that the lateral temperature gradient produced by the interference pattern plays a fundamental role in the facet formation.

A further interesting feature of the LIC process is the considerable amount of mass transport along the surface, which must occur while the material is in the liquid phase. The mass transport takes place in the direction of the temperature gradient created by the laser interference pattern, i.e., from regions of low temperature to regions of high temperature.

In the laser crystallization process discussed here, the epitaxial film grows from the liquid phase created by laser absorption. The LIC process differs from the conventional liquid phase epitaxy (LPE) due to the selective melting of the amorphous film and to the short melting and cooling times, which favor nonequilibrium processes. In the conventional LPE of Ge, (111)-faceted regions tend to appear on films grown on (100) and on (110) surfaces, while growth on (111) surfaces leads to smooth surfaces.[17] The formation of (111) faceted Ge crystals in the former case has been attributed to the higher surface energy of the (100) and (110) surfaces (of 1.57 and 1.42 J/m^2, respectively), relative to the (111) surface (1.12 J/m^2).[18] Based on these results, we expect the surface energy of (n11) surfaces to decrease when n decreases from ∞ [corresponding to the (100) surface] to 1 [(111) surface] and then to increase again when n goes to 0 [(110) surface]. In addition to these thermodynamic considerations, nonequilibrium phenomena associated with the short cooling times are also expected to play a fundamental role on the determination of the surface morphology. In fact, while slow growth rates favor the formation of faceted surfaces, rapidly growing surfaces from strongly undercooled liquids tend to be smooth.[19]

The previous considerations lead us to the following model for the formation of LIC lines with faceted surfaces. In the low fluency regime, the cooling times are short since only a small region of the Ge film melts and heat is quickly extracted through the interface with the substrate. The short cooling times prevent lateral material transport and also the formation of faceted crystals, so that the material crystallizes as a smooth film, as indicated in Fig. 4(a). The width of the molten region, as well as the cooling times, increases with laser fluency. In this case, the temperature gradient along the surface may then induce the lateral solidification process illustrated schematically in Fig. 6 for moderate (left panel) and for high (right panel) laser fluencies. The longer cooling times allow for lateral mass transport in the melt and favors the formation of faceted surfaces during solidification. The lateral mass transport is probably driven by the surface tension of the liquid, which tends to concentrate material close to the laser interference maxima, as illustrated in Figs. 6(b) and 6(e). In fact, surface tension has been shown to be an effective way of modeling the shape of microscopic silicon

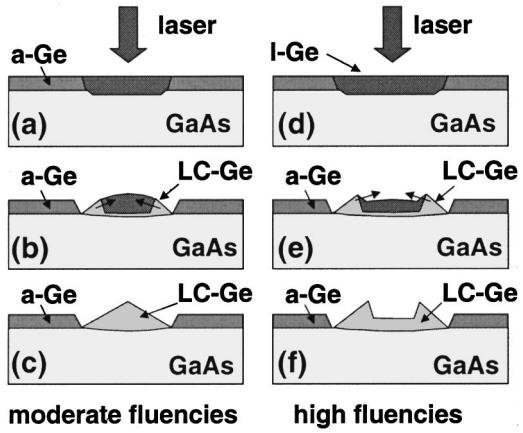

FIG. 6. Schematic sequence of events during the LIC process for moderate (left panel) and high laser fluencies (right panel) showing the selective laser melting [(a) and (d)], the lateral growth [(b)–(e)], and the final structure of the samples [(c)–(f)].

lines molten by pulsed laser irradiation.[20,21] The convex cross section of the liquid may also play a role in the determination of the final morphology of the surfaces after solidification.

The temperature gradient along the surface in Figs. 6(b) and 6(e) is such that the solidification starts from the border of the molten region and proceeds towards its center. The two crystallization fronts indicated in the figures leave behind well-defined faceted surfaces with a low surface energy. Since the melt is expected to wet the solidification fronts, the thickness of the solidified film increases as the front propagates. If the lateral fronts meet at the center of the lines before the molten material is consumed, the Ge lines will assume the triangular shape illustrated in Fig. 6(c). Since the width of the molten region increases with laser fluency, the liquid material may be consumed before the crystallization fronts meet at the center of the lines. In this case, lines with a trapezoidal-like cross section and with a depression in the center are obtained, as shown in Fig. 6(f).

According to the model described above, the lateral solidification process that leads to surface faceting requires a strong temperature gradient on the sample surface after the laser irradiation. The temperature distribution depends on the ratio between the laser pulse width and the characteristic time for lateral heat conduction along the surface. Large temperature gradients are unlikely to occur in short-period grating since the lateral heat conduction increases with decreasing grating period. Furthermore, large temperature gradients are not expected for very high fluencies, since these will be quickly smoothened by the thick and highly thermal conductive liquid film formed on the sample surface. Faceting is thus expected to become less pronounced for high laser fluencies, in agreement with the results in Fig. 1(d).

In conclusion, we have investigated the LIC of *a*-Ge films on (100) GaAs substrate. We demonstrate that the selective heating induced by the LIC process can be used to fabricate lines of epitaxial Ge films on GaAs. The lines have a faceted surface morphology, which depends on laser fluency. The latter is attributed to the lateral solidification in-

duced by the temperature gradient produced by the light interference pattern.

ACKNOWLEDGMENTS

The authors thank L. Däweritz for comments and for a critical reading of the manuscript and I. Poppe for the assistance in the SEM measurements. Support from the agencies Deutsche Akademischer Austauschdienst (DAAD, Germany) and CAPES (Brazil) is gratefully acknowledged.

[1] *Laser Annealing of Semiconductors*, edited by J. M. Poate and J. W. Mayer (Academic, New York, 1982).
[2] M. Heintze, P. V. Santos, C. E. Nebel, and M. Stutzmann, Appl. Phys. Lett. **64**, 3148 (1994).
[3] G. Aichmayr, D. Toet, M. Mulato, P. V. Santos, A. Spagenberg, S. Christiansen, M. Albrecht, and H. P. Strunk, Phys. Status Solidi A **166**, 659 (1998).
[4] G. Aichmayr, D. Toet, M. Mulato, P. V. Santos, A. Spagenberg, S. Christiansen, M. Albrecht, and H. P. Strunk, J. Appl. Phys. **85**, 4010 (1999).
[5] M. Mulato, D. Toet, G. Aichmayr, P. V. Santos, and I. Chambouleyron, Appl. Phys. Lett. **70**, 3570 (1997).
[6] M. K. Kelly, C. E. Nebel, M. Stutzmann, and G. Böhm, Appl. Phys. Lett. **68**, 1984 (1996).
[7] B. Rezek, C. E. Nebel, and M. Stutzmann, J. Non-Cryst. Solids **266**, 650 (2000).
[8] B. Rezek, C. E. Nebel, and M. Stutzmann, J. Non-Cryst. Solids **266**, 315 (2000).
[9] P. V. Santos, A. Trampert, F. Dondeo, D. Comedi, H. J. Zhu, K. H. Ploog, A. R. Zanatta, and I. Chambouleyron, J. Appl. Phys. **90**, 2575 (2001).
[10] R. Osório, S. Froyen, and A. Zunger, Phys. Rev. B **43**, 14055 (1991).
[11] D. Comedi, F. Dondeo, I. Chambouleyron, Z. L. Peng, and P. Mascher, J. Non-Cryst. Solids **266**, 713 (2000).
[12] *Landolt-Börnstein Tables Vol. 17c*, edited by H. W. O. Madelung and M. Schulz (Springer-Verlag, Heidelberg, 1984).
[13] R. Messier, T. Takamori, and R. Roy, Solid State Commun. **16**, 311 (1975).
[14] K. M. Lui, K. P. Chik, and J. B. Xu, Appl. Phys. Lett. **70**, 865 (1997).
[15] R. Turan, D. D. Perovic, and D. C. Houghton, Appl. Phys. Lett. **69**, 1593 (1996).
[16] J. R. Abelson, T. W. Sigmon, K. B. Kim, and K. H. Weiner, Appl. Phys. Lett. **52**, 230 (1988).
[17] M. Albrecht, P. O. Hansson, S. Christiansen, W. Dorsch, and H. P. Strunk, Scanning Microsc. **8**, 925 (1994).
[18] P. O. Hansson, M. Albrecht, W. Dorsch, H. P. Strunk, and E. Bauser, Phys. Rev. Lett. **73**, 444 (1994).
[19] D. Li and D. M. Heslach, Phys. Rev. Lett. **77**, 1801 (1996).
[20] T. Sameshima, Jpn. J. Appl. Phys., Part 2 **32**, L1485 (1993).
[21] G. Groos and M. Stutzmann, J. Non-Cryst. Solids **266**, 938 (1998).